The mechanism of neutral red-mediated microbial electrosynthesis in *Escherichia coli*: menaquinone reduction

Timothy D. Harrington, Vi N. Tran, Abdelrhman Mohamed, Ryan Renslow, Saeid Biria, Lisa Orfe, Douglas R. Call, Haluk Beyenal

PII: S0960-8524(15)00827-5
DOI: http://dx.doi.org/10.1016/j.biortech.2015.06.037
Reference: BITE 15116

To appear in: *Bioresource Technology*

Received Date: 2 April 2015
Revised Date: 4 June 2015
Accepted Date: 5 June 2015

Please cite this article as: Harrington, T.D., Tran, V.N., Mohamed, A., Renslow, R., Biria, S., Orfe, L., Call, D.R., Beyenal, H., The mechanism of neutral red-mediated microbial electrosynthesis in *Escherichia coli*: menaquinone reduction, *Bioresource Technology* (2015), doi: http://dx.doi.org/10.1016/j.biortech.2015.06.037

The mechanism of neutral red-mediated microbial electrosynthesis in *Escherichia coli*: menaquinone reduction

Timothy D. Harrington[1], Vi N. Tran[1], Abdelrhman Mohamed[1], Ryan Renslow[2], Saeid Biria[1,†], Lisa Orfe[3], Douglas R. Call[3], and Haluk Beyenal[1]*

[1]The Gene and Linda Voiland School of Chemical Engineering and Bioengineering, Washington State University, Pullman, WA, USA
[2]Environmental Molecular Sciences Laboratory, Pacific Northwest National Laboratory, Richland, WA, USA
[3]Paul G. Allen School for Global Animal Health, Washington State University, Pullman, WA, USA
[†]Present Address: Department of Biomedical and Chemical Engineering, Syracuse University, Syracuse, NY 13210, USA

Short running title: Neutral red microbial electrosynthesis mechanism

* Corresponding author. Email: beyenal@wsu.edu
Phone: 509-335-6607

ABSTRACT

The aim of this work was to elucidate the mechanism of mediated microbial electrosynthesis via neutral red from an electrode to fermenting *Escherichia coli* cultures in a bioelectrochemical system. Chemical reduction of NAD^+ by reduced neutral red did not occur as predicted. Instead, neutral red was shown to reduce the menaquinone pool in the inner bacterial membrane. The reduced menaquinone pool altered fermentative metabolite production via the *arcB* redox-sensing cascade in the absence of terminal electron acceptors. When the acceptors DMSO, fumarate, or nitrate were provided, as many as 19% of the electrons trapped in the reduced acceptors were derived from the electrode. These results demonstrate the mechanism of neutral red-mediated microbial electrosynthesis during fermentation as well as how neutral red enables microbial electrosynthesis of reduced terminal electron acceptors.

Keywords: Neutral red, electron transfer, bioelectrochemical system, microbial electrosynthesis, menaquinone

1. Introduction

Among the developing Microbial Electrochemical Technologies (METs), the use of redox mediators to transport electrons to or from microorganisms has received considerable attention due to its potential to uncouple energy metabolism from growth (Clark et al., 2012) and to alter terminal metabolite production toward more valuable products during fermentation (Emde and Schink, 1990; Hongo and Iwahara, 1979; T. Kim and B. Kim, 1988; S. M. Park et al., 2005; Peguin et al., 1994) in a process that has been called both "microbial electrosynthesis" (Patil et al., 2015; Schröder et al., 2015), and "electro-fermentation" (Rabaey and Rozendal, 2010). The delivery of electrons to fermenting cells for biocommodity production has been successfully implemented using several different mediators, including neutral red, benzyl viologen, methyl viologen, humic substances, and anthraquinone 2,6-disulfonate (Emde and Schink, 1990; Hongo and Iwahara, 1979; T. Kim and B. Kim, 1988; S. M. Park et al., 2005; Peguin et al., 1994). Among these, neutral red has shown promise due to its low toxicity and low standard reduction potential (E_o = −525 $mV_{Ag/AgCl}$) (Hongo and Iwahara, 1979; D. H. Park and Zeikus, 1999).

Neutral red (3-Amino-7-dimethylamino-2-methylphenazine hydrochloride) is a cationic dye that is commonly used as a histological stain because of its optical sensitivity to pH in the physiologically relevant range of pH 6.0-8.0 (Halliday and Matthews, 1983). Although it is water-soluble, it has a lipid/water partition coefficient of 30 (LaManna and Lauro, 1998), making it extremely hydrophobic. The structure of neutral red differs under different pH and redox potentials (Fig. S1, see Supplementary Information). These structures include neutral red (NRH^+), reduced neutral red (NRH_2), and leuco neutral red (NR).

When dissolved in water at pH 7.0, the chloride salt of NRH^+ makes a red-colored solution. Raising the pH to 8.0 or dissolving the salt in octanol yields a yellow-colored solution. Electrochemical reduction in water yields a yellow solution with a green fluorescence. Reduction of NRH^+ and NR occurs via two-electron transfer (Azariah et al., 1998) at a standard potential ($E_o = -525mV_{Ag/AgCl}$ for NRH_2/NRH^+) that is close to the standard potential of the biological redox carrier nicotinamide adenine dinucleotide hydride ($E_o = -515mV_{Ag/AgCl}$ for $NADH/NAD^+$). NRH^+ is reduced to NRH_2 by a number of bacterial species, including *Escherichia coli* and *Klebsiella pneumonia* (Chamot and Sherwood, 1917; Gage and Phelps, 1902; Makgill, 1901), as well as by a polarized graphite electrode (D. H. Park and Zeikus, 1999). Neutral red interacts with bacteria by accepting electrons from hydrogenase for delivery to dissolved iron or to an anode in a microbial fuel cell (McKinlay and Zeikus, 2004). Neutral red can also shuttle electrons to cells via several proposed mechanisms (D. H. Park et al., 1999; D. H. Park and Zeikus, 1999). Previous research suggested that NRH_2 can alter bacterial metabolism by reducing nicotinamide adenine dinucleotide (NAD^+) to NADH (D. H. Park and Zeikus, 1999). Others have demonstrated that NAD^+ reduction via NRH_2 could not have accounted for metabolic changes observed during neutral red-mediated electrosynthesis (Harrington et al., 2015. The hypothesis of the present work is that the previously observed effects may have rather been caused by a gene regulation mechanism, as opposed to stoichiometric delivery of extra electrons that are trapped in terminal metabolites. Herein spectroscopic and electrochemical techniques were used to investigate the supposed reaction whereby NRH_2 reduces NAD^+.

An alternative hypothesis proposed that NRH_2 might take the place of menaquinone (MK) in the fumarate reductase complex during the microbial electrosynthesis of succinate from fumarate.

Park and Zeikus demonstrated that electrons could be supplied to fumarate reductase for fumarate reduction in *Actinobacillus succinogenes* when both NRH_2 and fumarate were present (D. H. Park and Zeikus, 1999). Previous experiments in the authors' laboratory showed that when an electron acceptor was provided to the catholyte during electrosynthesis, the magnitude of the current delivery differed significantly relative to the same experiment when no electron acceptor was provided. In the former, the magnitude of current was high and the transferred electrons could be accounted for via production of succinate. For the latter, the change in final product concentration (lactate, ethanol, etc.) was significant, but could not be sufficiently explained by the current magnitude (Harrington et al., 2015). A single mechanism was proposed to be behind the ability of neutral red to alter product formation and the ability of neutral red to reduce fumarate in the fumarate reductase complex. The hypothesis was that neutral red directly reduces menaquinone to menaquinol (MKH_2) as opposed to taking its place, which would sufficiently explain the increased fumarate reduction, as well as the fermentation profile changes observed when no electron acceptor was provided, by means of the recently elucidated redox-sensing arc signal transduction pathway.

The arc (**a**erobic **r**espiratory **c**ontrol) pathway alters a cell's response to its redox environment via a membrane-associated protein called ArcB, and a transcriptional regulator called ArcA (Alvarez et al., 2013). The arc cascade alters expression of hundreds of genes in *E. coli* in direct response to quinone redox states (Salmon et al., 2005), which could explain the altered protein expression profiles observed previously during neutral red-mediated electrosynthesis experiments (Harrington et al., 2015). To test this hypothesis, microbial electrosyntheses were performed with and without the terminal electron acceptors fumarate, DMSO, and nitrate using *E.*

coli strains that were deficient in anaerobic quinone production (*menA* null mutants, deficient in both menaquinone and demethylmenaquinone) as well as *arcB* null mutants, and their complement strains. Overall, neutral red-mediated microbial electrosynthesis was shown to alter fermentation profiles, cause the reduction of terminal metabolites like DMSO, fumarate and nitrate, as well as drive energy-conserving respiration in combination with nitrate reduction.

2. Materials and methods

2.1 Bacterial strains

E. coli K-12 strains JW5536 (Δ*arcB*) and JW3901 (Δ*menA*) were selected from the Keio collection (Baba et al., 2006). Disruption of the *menA* gene results in the inability to produce demethylmenaquinone and menaquinone while leaving intact the ability to produce ubiquinone. Complementation (JW5536(pMMB207::*arcB*) and JW3901(pMMB207::*menA*)) was achieved using the low copy expression plasmid pMMB207 (ATCC 37809). Briefly, primers AGTCGAATTCATGACTGAACAACAAATTAGCCGAA (*menA*_forward_*EcoRI*), AGTCGTCGACTTAATGATGATGATGATGTGCTGCCCACTGGCTTAGG (*menA*_reverse_*SalI*), AGTCGAATTCATGAAGCAAATTCGTCTGCTGG (*arcB*_forward_*EcoRI*), and AGTCGTCGACTCAATGATGATGATGATGTTTTTTAGTGGCTTTTGCCACCC (*arcB*_reverse_*SalI*) were used to amplify the *menA* and *arcB* genes from *E. coli* genomic DNA. The amplicons were digested and ligated into pMMB207 and the resulting construct was electroporated into competent *E. coli* S-17 cells and selected on chloramphenicol(Zhou et al., 2008). Constructs were confirmed via sequencing, then electroporated into their respective

competent mutant strains and selected on kanamycin/chloramphenicol. Expression was induced with 50 μM (*arcB*) or 10 μM (*menA*) isopropyl β-D-1-thiogalactopyranoside (IPTG) where indicated.

2.2 Fermentation media

Unless otherwise noted chemicals were obtained from Fisher Scientific. Fermentation without an electron acceptor was performed in media composed of the following, L^{-1}: M-9 salts 5×, 200 mL; $MgSO_4$ (1 M), 2 mL; $CaCl_2$ (1 M), 100 μL); yeast extract, 5 g, Difco; D-glucose, 20 g. Neutral red (200 μM; CAS: 553-24-2, Sigma) was included to deliver electrons to growing cells except during control experiments. Antibiotics were included where necessary. Neutral red was prepared as a 20× stock solution, vacuum filtered with a 0.2 μm membrane, and added to the separately filtered media. Experiments that included electron acceptors were performed in the same media, except with 2.5 g yeast extract, no D-glucose, and the addition of one of either sodium nitrate (20 mM), dimethyl sulfoxide (DMSO, 20 mM), or sodium fumarate (20 mM).

2.3 Bioelectrochemical reactors

Adams and Chittenden (Berkeley, CA, USA) 100 mL microbial fuel cells with VICI-Jour (Schenkon, Switzerland) bottle caps and Eldon James (Denver, CO, USA) bulkhead fittings (BH-1428-2-2NK) were operated as batch bioelectrochemical reactors (BERs). A Membranes International (Ringwood, NJ, USA) cation exchange membrane (CMI-7000) separated the two 100 mL chambers. One side was filled with 100 mL fermentation media, and the other was filled with 100 mM sodium phosphate buffer, pH 7.0. A graphite rod (496553, Sigma) and lab-built Ag/AgCl reference electrode were suspended in the phosphate buffer. Graphite felt (HP

Materials Solutions, Inc., Woodland Hills, CA, USA) was cut into coupons (diameter = 2.2 cm, thickness = 6 mm) to serve as the cathodes and these were attached to titanium wire (Keegotech, Menlo Park, CA, USA). This electrode and a stir bar were inserted into the fermentation chamber. All three electrodes were connected to a single channel of a six-channel potentiostat developed previously (Renslow et al., 2011). The same reactors were used for control experiments without the inclusion of electrodes. Reactors were autoclaved, filled with sterile media, flushed with nitrogen, and reduced overnight. The working electrode was polarized to -650 $mV_{Ag/AgCl}$ overnight prior to inoculation and after inoculation to ensure complete and continuous reduction of the neutral red during the experiments. Starter cultures (50 mL, neutral red-free media) were grown anaerobically to an OD_{600} of 0.55 to 0.60, and 2.5 mL from these were inoculated into pre-reduced reactors. Samples of the fermentation broth were taken periodically. Stir bars were included in the fermentation chamber and rotated at 150 rpm.

2.4 Abiotic neutral red electrochemistry

NAD^+ reduction experiments were carried out in the same bioelectrochemical reactors as the fermentations. The cathode compartments were filled with continuously nitrogen-sparged, phosphate buffered (100 mM) solutions of 200 μM neutral red at pH 6.0, and pre-reduced overnight using a polarized graphite felt electrode. The graphite electrodes were polarized to −650 $mV_{Ag/AgCl}$ or −950 $mV_{Ag/AgCl}$ to test both reduction states of neutral red. The current was allowed to reach steady state (~ -35 μA) and was monitored over time. A nitrogen-flushed solution of 2 M NAD^+ in water was injected to the pre-reduced solution to a final concentration of 200 μM NAD^+. Samples (1 ml) were subsequently taken at intervals for absorbance measurements. Similar experiments were performed in which sonication-lysed *E. coli* cells were

suspended in the neutral-red solution within a dialysis membrane to determine if cellular proteins could catalyze NAD^+ reduction by neutral red. As a positive control (Steuber et al., 1999), the same NAD^+ solution was injected into a freshly prepared anaerobic solution of sodium dithionite (200 μM, standard reduction potential = -858 $mV_{Ag/AgCl}$) and absorbance was monitored at intervals.

2.5 Analytical Techniques

Fermentation samples (0.7 mL) were assayed for absorbance (OD_{650}) to track cell growth using an Agilent 8410 UV-VIS spectrophotometer. The wavelength 650 nm was chosen because it is outside the absorbance spectrum of neutral red. After assaying cell growth, samples were centrifuged and the supernatants were analyzed for metabolite concentrations with an Agilent 1100 HPLC equipped with diode array and refractive index detectors.

Cyclic voltammograms (CVs) and chronoamperometry plots were obtained with a Gamry 300 potentiostat and lab-built six-channel potentiostat, respectively, using a Ag/AgCl reference electrode. All potentials are reported with respect to this reference. Where indicated, chronoamperometry plots were integrated using an interpolating function in Mathematica(Wolfram Research, Inc., 2012) version 9.0.1.0 (Wolfram Research) and charge transferred was converted to the equivalent of mM of 2-electron pairs for simple comparison to metabolite concentrations. Mathematica© was also used to perform the student's t-test to determine the significance of differences observed for fermentation end-product concentrations. All biotic and abiotic experiments were conducted with at least two independent replicates. Single spectra or chromatograms are presented for clarity.

3. Results and discussion

3.1 Neutral red and NAD^+ reduction

The published electrochemical experiments that previously linked reduced NR with NAD^+ reduction used a high potential drop (2000 mV) to reduce the NR without controlling the working electrode potential with a potentiostat (Jeon et al., 2012; D. H. Park and Zeikus, 1999). In addition, the solutions may have not been pre-reduced before adding NAD^+. Because neutral red is known to undergo multiple redox reactions, cyclic voltammetry was performed with a large potential window (−1200 to +500 $mV_{Ag/AgCl}$) to determine which species may have been responsible for NAD^+ reduction. While performing the scans on a phosphate buffered neutral red solution, two cathodic peaks with corresponding anodic peaks were observed (Fig. 1A). The first peak is the most commonly discussed reversible peak, which had a midpoint potential of -504 $mV_{Ag/AgCl}$ and a cathodic peak voltage (V_{pc}) of -566 $mV_{Ag/AgCl}$. This measured midpoint potential is within 9 mV of the published value for neutral red at pH 6.0 (Fig. S1). The second peak had a more positive midpoint potential of -346 $mV_{Ag/AgCl}$, but with a much larger overpotential, demonstrated by the V_{pc} of -909 $mV_{Ag/AgCl}$. This second reduction peak was noted by Halliday et al. (Halliday and Matthews, 1983), but has received little attention in the literature. Constant polarization on the cathodic side of both peaks (-650 $mV_{Ag/AgCl}$ and -950 $mV_{Ag/AgCl}$) yielded two solutions with different optical absorbance spectra (Fig. 1B). These two molecules are referred to in this work as NRH_2 and NR_{-950}, respectively.

Interestingly, NR_{-950} had a peak absorbance at 335 nm and overlapped significantly with the wavelength used to detect NADH (340 nm). This indicates that the unintentional reduction of NR to NR_{-950} may have served as a false positive for NAD^+ reduction in previous work (D. H. Park and Zeikus, 1999). Therefore, solutions of both NRH_2 and NR_{-950} were tested the ability to reduce NAD^+ after the neutral red had been pre-reduced (Fig. S2, see Supplementary Information).

Addition of NAD^+ to pre-reduced neutral red solutions did not result in the production of NADH as observed by the absorbance change at 340 nm (Fig. S2A and S2B). Absorbance values did not change for at least 180 min. Furthermore, no current change was observed during continuous polarization of neutral red solution after NAD^+ addition, indicating that neutral red was not being oxidized by NAD^+ and that NAD^+ was not being reduced by the electrode (data not shown). As a positive control the same solution of NAD^+ was injected to a final concentration of 200 μM into a freshly prepared anaerobic solution of 200 μM sodium dithionite (Fig. S2C). The absorbance peak corresponding to sodium dithionite (315 nm) began to disappear almost immediately while the peak corresponding to NADH (340 nm) began to increase. To determine if an enzyme could catalyze the reduction of NAD^+ by NRH_2, sonicated and concentrated *E. coli* lysate was suspended in a dialysis bag. This material was then included in a cathode that was full of continuously reduced NRH_2, but NADH production was not observed within 24 h (data not shown).

Given these results, the authors surmise that the previous conclusion that NRH_2 can reduce NAD^+ to NADH was made because of the unexpected generation of NR_{-950}, which has an

overlapping absorbance spectrum with NADH. Taken together with the previous observation that there is insufficient current delivered to electrosynthesizing cells for NAD^+ reduction to be the mechanism (Harrington et al., 2015), the conclusion was reached that NAD^+ was not reduced by electrons derived from the electrode.

3.2 Role of arcB in neutral red-mediated microbial electrosynthesis

Neutral red is extremely hydrophobic and it binds to cell membranes (D. H. Park and Zeikus, 1999); our results indicate that neutral red does not reduce NAD^+. Consequently, the hypothesis that NRH_2 can affect the redox-sensing mechanism in *E. coli* was tested. This was accomplished by comparing control (non-polarized, no neutral red) vs. electrosynthesis (polarized at -650 $mV_{Ag/AgCl}$, with neutral red) metabolite profiles in wild-type *E. coli* K-12, strain JW5536 (Δ*arcB*), and its complement strain JW5536 (pMMB207::*arcB*). The *arcB* deletion altered multiple metabolite profiles including formation of pyruvate and formate, but the effect is best illustrated by lactate profiles (Fig. 2).

Wild-type cells produced significantly more lactate (15%) at 15.5 hours during electrosynthesis vs. control ($P = 0.003$; Fig. 2A). The *arcB* mutant (Fig. 2B) showed changes in the shape of the fermentation profiles and final concentrations when compared to the wild-type strain (Fig. 2A), but resulted in no difference between electrosynthesis and control conditions in fermentation profiles or final concentration for lactate or any of the other terminal metabolites, including acetate, formate, succinate, pyruvate, and ethanol (data not shown). Complementation of the *arcB* gene on the pMMB207 plasmid was verified by sequencing, but an appropriate level of expression proved difficult. IPTG induction is normally performed on aerobic cultures during

exponential growth. After inducing with 50 μM IPTG, growth and metabolite production were significantly retarded, presumably due to the metabolic resources that were diverted to drive expression of *arcB* on the plasmid (Bienick et al., 2014) (Fig. 2C). Nevertheless, a higher final lactate concentration (40% higher vs. control) could still be observed in the electrosynthesis reactors at 15.5 h. Because *arcB* was required to effect a change during electrosynthesis with NRH_2, the hypothesis that metabolism is altered by NRH_2 via redox-sensing, as opposed to NAD^+ reduction, was supported. This result did not determine, however, if *arcB* was reduced directly by NRH_2, or via an intermediate (e.g. menaquinone).

3.3 Role of menaquinone in microbial electrosynthesis with neutral red

To test whether menaquinone was involved in the oxidation of neutral red, fumarate (20 mM) was added to the media of electrosynthesis BERs prior to the initial overnight pre-reduction by the potentiostat. The current for the wild-type strain peaked at −1.3 mA (Fig. 3A). When integrated the amount of current delivered in the presence of fumarate was 2.86 mM of equivalent 2-electron pairs, vs. 0.27 mM when no fumarate was added (Harrington et al., 2015). This one order-of-magnitude difference indicated that fumarate served as an electron sink by oxidizing NRH_2 and the profile indicated that the reaction was associated with cell concentration. Cell growth ceased at six hours post-inoculation.

When neutral red was omitted from the reactor, no current was observed, and when the *menA* mutant strain JW3901(Δ*menA*) was tested, the current profile did not change in response to growth. The only change was a slow decrease over time in background current due to slow evaporation of the water and concentration of neutral red in the media. The total charge transferred to the *menA* mutant strain was 0.20 mM, comparable to the value for wild type when

no fumarate was added. When *menA* was complemented (JW3901(pMMB207::*menA*)) it was extremely sensitive to even low IPTG concentration (10 μM IPTG induction at 1 h post-inoculation) when the reactor contained low cell counts early in the fermentations. Nevertheless, a partially restored current profile was observed vs. the mutant current profile (Fig. 3A) consistent with menaquinone mediating the oxidation of neutral red by fumarate. The essential role of menaquinone in neutral red-mediated electrosynthesis may explain the lack of an effect seen previously on the bacterium *Zymomonas mobilis* (Harrington et al., 2015) because *Z. mobilis* does not produce menaquinone (Strohdeicher et al., 1990).

3.4 Alternative electron acceptors

Because menaquinone and demethylmenaquinone are known to drive anaerobic respiration for a variety of electron acceptors in *E. coli* (Sharma et al., 2012), electrosyntheses were performed with the inclusion of sodium nitrate (20 mM) and DMSO (20 mM) to test whether neutral red could drive these alternate respiration pathways in the *E. coli* inner membrane. The results are shown in Fig. 3B, together with the fumarate profile from Fig. 3A.

Peak currents of −1.25, −1.29, and −0.77 mA were delivered to cells grown with nitrate, fumarate, and DMSO, respectively, all of which use menaquinone and/or demethylmenaquinone as their electron donors. Menaquinone is normally reduced to menaquinol (MKH_2) via a proton-pumping NADH dehydrogenase (i.e. nuo or Complex I), resulting in proton-translocation across the inner membrane and regeneration of menaquinone after oxidation by a terminal electron acceptor. In prokaryotes the oxidation of NADH by NADH dehydrogenase is the reaction step that contributes the most to proton motive force. When menaquinone is reduced by neutral red there is no resulting proton translocation and therefore no generation of proton motive force

(pmf). This is likely the mechanism by which electrosynthesis with each of these acceptors resulted in lower final optical densities at 650 nm vs. control (fumarate: 0.42 vs. 0.52, DMSO: 0.40 vs. 0.57, nitrate: 0.85 vs. 1.06). By reducing menaquinone, neutral red took the place of the pmf-generating reduction of menaquinone by NADH, resulting in lower ATP yields and lower biomass generation vs. the control fermentation with the same acceptor. In effect, neutral red "robbed" the electron transport chain of energy that could have been used to generate ATP. In *E. coli*, nitrate reduction yields more energy than the other electron acceptors because the respiratory nitrate reductase (nar) contributes to pmf (Sparacino-Watkins et al., 2013), leading to higher ATP yields and higher final biomass concentrations. As such, the nitrate-reducing reactors grew faster vs. the fumarate- and DMSO-containing reactors, attaining higher cell densities and more rapid nitrate reduction. Nitrate was thus depleted within 8.5 hours, whereas DMSO and fumarate were not yet completely depleted at 15.5 hours.

Integration of the current delivered to the reactors in Fig. 3B and conversion of the values to concentrations of two-electron pairs gave 1.35 mM, 1.68 mM, and 2.86 mM two-electron pair equivalents delivered to nitrate- (8.5 hours), DMSO- (15.5 hours), and fumarate- (15.5 hours) containing media, respectively. Quantification of metabolites using HPLC showed that 20 mM nitrate, 10 mM DMSO, and 15.1 mM fumarate were reduced by 8.5, 15.5, and 15.5 hours, respectively. Thus, neutral red was the electron source for 6.7% of the nitrate reduced, 16.8% of the DMSO reduced, and 18.9% of the fumarate reduced during the electrosynthesis. In all cases, the majority of the electrons that moved through menaquinol to a terminal reductase were derived from a source internal to the cell, most likely NADH via type I NADH dehydrogenase. When nitrate concentration dropped below our limit of detection (0.5 mM) at 8.5 h, the current

remained at ~ -0.5 mA, most likely due to the commencement of nitrite reduction. *E. coli* is known to preferentially reduce nitrate with the stoichiometry $1MKH_2 + 1NO_3^- \rightarrow 1MK + 1NO_2^-$, followed by a switch to nitrite reduction (Lin and Iuchi, 1991), with the stoichiometry $3MKH_2 + 1NO_2^- \rightarrow 3MK + 1NH_4$ (Abou-Jaoude et al., 1979).

3.4 Proposed mechanism of neutral red-mediated microbial electrosynthesis

Though it is possible that NRH_2 may be involved in alternative reactions, as recently demonstrated for anthraquinone-2,6-disulfonate (AQDS) (Clark et al., 2012), the data presented here demonstrate that the major reaction is the reduction of menaquinone to menaquinol in the inner membrane of *E. coli* (Fig. 4).

3.4.1 Physiology of the neutral red mechanism

NRH_2 has at least two effects on growing *E. coli* culture, both of which are a direct consequence of the ability of neutral red to reduce menaquinone (step 3, Fig. 4). During fermentation conditions (no electron acceptor) neutral red can drive the menaquinol/menaquinone pool to a more reduced state than normally obtained by cellular metabolism alone. The reduced menaquinone pool modulates the activation of the ArcB/ArcA cascade, ultimately resulting in transcriptional changes to genes with ArcA recognition sites. The changes in terminal metabolites observed during fermentation conditions are not stoichiometrically related to the faradaic current delivered during neutral red-mediated electrosynthesis, and the delivered electrons are not trapped in the resulting fermentation products. However, when a terminal electron acceptor *is* provided, neutral red continuously

supplies the menaquinone pool with electrons, resulting in stoichiometric microbial electrosynthesis of the reduced terminal electron acceptor from the oxidized form.

When the terminal reductase employed is like fumarate reductase and does not cause proton translocation, this process is a futile cycle that does not generate proton motive force. With nitrate reductase, however, menaquinol protons are released to the periplasm and nitrate consumes protons from the cytoplasm. This process results in proton motive force that could be used to drive membrane enzymes like ATP synthase and transhydrogenase. Neutral red reduction of menaquinone competes with the normal biological reduction by NADH, which does move protons via Type I NADH dehydrogenase. Therefore, for every pair of neutral red-derived electrons that end up in the terminal electron acceptor, there is less proton motive force available to do work than if all of the electrons were derived from NADH.

3.4.2 Thermodynamics and optimization of menaquinone reduction

Based on previous results comparing electrosynthesis to control fermentations (Harrington et al., 2015) and the mechanism reported here, the authors propose that electrosynthesis with neutral red results in a "more anaerobic" phenotype during fermentation as a direct consequence of the "over-reduction" of the menaquinone pool. The ability of neutral red to over-reduce the menaquinone pool when compared to its usual source of electrons (NADH) is a direct consequence of the mechanisms and thermodynamics of the two separate processes. The $NADH/NAD^+$ ratio only approaches 0.75 in fermenting *E. coli* cells (de Graef et al., 1999) and the electrons in NADH lose part of their energy in pumping protons through type I NADH dehydrogenase, nuo (non-proton pumping type II NADH dehydrogenase, ndh, is repressed during anaerobic growth) (Spiro et al., 2006). Neutral red has a slightly lower standard redox

potential (−525 $mV_{Ag/AgCl}$) vs. the NADH couple (-515 $mV_{Ag/AgCl}$), and its actual potential is even lower when the electrode is used to keep the NRH_2/NRH^+ ratio high (>1). Because it does not spend this energy transporting protons, NRH_2 is able to drive the menaquinone pool (-271 $mV_{Ag/AgCl}$) to a more reduced state. By reducing the menaquinone pool, neutral red-mediated electrosynthesis may cause a slight increase in the $NADH/NAD^+$ ratio by blocking a slow, "leaky" flux of NADH electrons that may end up in menaquinone associated redox reactions when minimal quantities of electron acceptors are present. In the case of *E. coli*, fumarate is normally reduced to succinate with a menaquinol whose electrons derive from NADH. If this reduction were to be driven by neutral red, the NADH molecule is then free to be used for other reductive processes. This mechanism may explain why electrosynthesis often results in higher concentrations of reduced metabolites, besides the accounting for changes in gene expression (Harrington et al., 2015; Choi et al., 2014).

Even though neutral red draws a large current in the presence of a terminal electron acceptor during cell growth, the rates of NRH_2 oxidation by menaquinone and re-reduction of NRH^+ by the electrode change over time. A comparison of the *rates* of menaquinone reduction by NADH and neutral red was not obtained. The fact that no more than 19% of the electrons delivered to the terminal electron acceptors were derived from neutral red suggests that the NADH route is faster, but this may change with higher neutral red concentration, substrate-limiting conditions, better mixing, and/or optimization of the BER to minimize the average distance that neutral red must travel between bacterial cells and the electrode. In addition, the time lag between NRH_2 oxidation to NRH^+ by menaquinone and re-reduction of the NRH^+ to NRH_2, as well as the potential for some neutral red to remain in the membrane after oxidation may have led to an

underestimation of the percent of electrons that are derived from neutral red. The optimization of the rate of reduction of menaquinone with externally derived electrons via neutral red will be addressed in future research.

Using several lines of evidence, the conclusion was reached that neutral red reduces menaquinone with electrons derived from the electrode. The resulting reduced menaquinone pool causes regulatory changes in the absence of a terminal electron acceptor via the arcB/arcA "**a**erobic **r**espiratory **c**ontrol" cascade. In the presence of an anaerobic terminal electron acceptor, menaquinone is rapidly oxidized and subsequently re-reduced by neutral red. Thus, neutral red can "trick" the cells' interpretation of their redox state by uncoupling the menaquinol/menaquinone redox state from the NADH/NAD^+ redox state. In combination with the necessary terminal reductase, NRH_2 can drive the reduction of anaerobic, terminal electron acceptors including fumarate, DMSO, nitrate, and nitrite via menaquinone, independent from cytoplasmic electron carriers like NADH that derive from the carbon source.

4. Conclusions

The mechanism of action and effects of neutral red-mediated electrosynthesis on *E. coli* metabolism were demonstrated. NRH_2 was shown to reduce menaquinone in the inner membrane. The over-reduced menaquinone pool alters the redox state of the arcB sensor protein, resulting in altered metabolite profiles. NRH_2 can partially drive anaerobic respiration with the electron acceptors fumarate, nitrate, DMSO, and nitrite. An NRH_2/NO_2 external respiration scheme could be used to generate proton motive force and eliminate the need to oxidize NADH in order to drive respiration.

Acknowledgements

This work was supported by NSF Career Award 0954186, and TDH was partially supported by NIH Training Grant 5T32GM008336-24. The authors thank Jerome T. Babauta for his instrumental advice in the preparation of this manuscript. RSR acknowledges the Environmental Molecular Sciences Laboratory (EMSL), a national scientific user facility sponsored by the Department of Energy's Office of Biological and Environmental Research, and the Linus Pauling Distinguished Postdoctoral Fellowship at Pacific Northwest National Laboratory.

References

1) Abou-Jaoude, A., Chippaux, M., Pascal, M.-C., 1979. Formate□nitrite reduction in *Escherichia coli* K12. Eur. J. Biochem. 95, 309–314.
2) Alvarez, A.F., Rodriguez, C., Georgellis, D., 2013. Ubiquinone and menaquinone electron carriers represent the yin and yang in the redox regulation of the ArcB sensor kinase. J. Bacteriol. 195, 3054–3061. doi:10.1128/JB.00406-13
3) Azariah, A.N., Sheela, B., Yegnaraman, V., 1998. Electrochemical behaviour of neutral red. B Electrochem. 14, 309–314.
4) Baba, T., Ara, T., Hasegawa, M., Takai, Y., Okumura, Y., Baba, M., Datsenko, K.A., Tomita, M., Wanner, B.L., Mori, H., 2006. Construction of *Escherichia coli* K-12 in-frame, single-gene knockout mutants: the Keio collection. Mol. Syst. Biol. 2. doi:10.1038/msb4100050
5) Bienick, M.S., Young, K.W., Klesmith, J.R., Detwiler, E.E., Tomek, K.J., Whitehead, T.A., 2014. The interrelationship between promoter strength, gene expression, and growth rate. PLoS One 9, e109105. doi:10.1371/journal.pone.0109105.s008
6) Chamot, E.M., Sherwood, C.M., 1917. Studies on the culture media employed in the bacteriological examination of water. J. Am. Chem. Soc. 1755–1766.
7) Choi, O., Kim, T., Woo, H.M., Um, Y., 2014. Electricity-driven metabolic shift through direct electron uptake by electroactive heterotroph *Clostridium pasteurianum*. Sci. Rep. 4, 6961. doi:10.1038/srep06961
8) Clark, I.C., Carlson, H.K., Iavarone, A.T., Coates, J.D., 2012. Bioelectrical redox cycling of anthraquinone-2,6-disulfonate coupled to perchlorate reduction. Energy Environ. Sci. 5, 7970. doi:10.1039/c2ee21594b
9) de Graef, M.R., Alexeeva, S., Snoep, J.L., Teixeira de Mattos, M.J., 1999. The steady-state internal redox state (NADH/NAD) reflects the external redox state and is correlated with catabolic adaptation in *Escherichia coli*. J. Bacteriol. 181, 2351–2357.
10) Emde, R., Schink, B., 1990. Enhanced propionate formation by *Propionibacterium-Freudenreichii* Subsp. Freudenreichii in a three-electrode amperometric culture system. Appl. Environ. Microbiol. 56, 2771–2776.
11) Gage, S.D., Phelps, E.B.E., 1902. Notes on *B. Coli* and allied forms, with special reference to the neutral-red reaction. Public Health Pap. Rep. 28, 402–412.
12) Halliday, C.S., Matthews, D.B., 1983. Some electrochemical and photoelectrochemical properties of 3-Amino-7-dimethylamino-2-methylphenazine (neutral red) in aqueous solution. Aust. J. Chem. 507–516.
13) Hongo, M., Iwahara, M., 1979. Application of electro-energizing method to L-glutamic acid fermentation. Agric. Biol. Chem. 43, 2075–2081.
14) Jeon, B.Y., Jung, I.L., Park, D.H., 2012. Conversion of carbon dioxide to metabolites by *Clostridium acetobutylicum* KCTC1037 cultivated with electrochemical reducing power. Adv. Microbiol. 2, 332–339. doi:10.4236/aim.2012.23040
15) Kim, T., Kim, B., 1988. Electron flow shift in *Clostridium acetobutylicum* fermentation by electrochemically introduced reducing equivalent. Biotechnol. Lett. 10, 123–128.
16) LaManna, J.C., Lauro, K.L., 1998. pH and brain function. Wiley.
17) Lin, E.C.C., Iuchi, S., 1991. Regulation of gene expression in fermentative and respiratory systems in *Escherichia coli* and related bacteria. Genetics 25, 361–387. doi:10.1146/annurev.ge.25.120191.002045
18) Makgill, R.H., 1901. The neutral-red reaction as a means of detecting *Bacillus colin* in water

supplies. J Hyg (Lond) 1, 430–436. doi:10.1017/S0022172400000383
19) McKinlay, J.B., Zeikus, J.G., 2004. Extracellular iron reduction is mediated in part by neutral red and hydrogenase in *Escherichia coli*. Appl. Microbiol. Biotechnol. 70, 3467–3474. doi:10.1128/AEM.70.6.3467-3474.2004
20) Park, D.H., Laivenieks, M., Guettler, M.V., Jain, M.K., Zeikus, J.G., 1999. Microbial utilization of electrically reduced neutral red as the sole electron donor for growth and metabolite production. Appl. Environ. Microbiol. 65, 2912–2917.
21) Park, D.H., Zeikus, J.G., 1999. Utilization of electrically reduced neutral red by *Actinobacillus succinogenes*: physiological function of neutral red in membrane-driven fumarate reduction and energy conservation. J. Bacteriol. 181, 2403–2410.
22) Park, S.M., Kang, H.S., Park, D.W., Park, D.H., 2005. Electrochemical control of metabolic flux of *Weissella kimchii* sk10: neutral red immobilized in cytoplasmic membrane as electron channel. J. Microbiol. Biotechnol. 15, 80–85.
23) Patil, S.A., Gildemyn, S., Pant, D., Zengler, K., Logan, B.E., Rabaey, K., 2015. A logical data representation framework for electricity-driven bioproduction processes. Biotechnology Advances 1–9. doi:10.1016/j.biotechadv.2015.03.002
24) Peguin, S., Delorme, P., Goma, G., Soucaille, P., 1994. Enhanced alcohol yields in batch cultures of *Clostridium acetobutylicum* using a three-electrode potentiometric system with methyl viologen as electron carrier. Biotechnol. Lett. 16, 269–274.
25) Rabaey, K., Rozendal, R.A., 2010. Microbial electrosynthesis — revisiting the electrical route for microbial production. Nat. Rev. Microbiol. 8, 706–716. doi:10.1038/nrmicro2422
26) Renslow, R., Donovan, C., Shim, M., Babauta, J., Nannapaneni, S., Schenk, J., Beyenal, H., 2011. Oxygen reduction kinetics on graphite cathodes in sediment microbial fuel cells. Phys. Chem. Chem. Phys. 13, 21573–21584. doi:10.1039/c1cp23200b
27) Salmon, K.A., Hung, S.P., Steffen, N.R., Krupp, R., Baldi, P., Hatfield, G.W., Gunsalus, R.P., 2005. Global gene expression profiling in *Escherichia coli* K12: effects of oxygen availability and ArcA. J. Biol. Chem. 280, 15084–15096. doi:10.1074/jbc.M414030200
28) Schröder, U., Harnisch, F., Angenent, L.T., 2015. Microbial electrochemistry and technolog: terminology and classification. Energy Environ. Sci. 8, 513–519. doi:10.1039/C4EE03359K
29) Sharma, P., Teixeira de Mattos, M.J., Hellingwerf, K.J., Bekker, M., 2012. On the function of the various quinone species in *Escherichia coli*. FEBS J 279, 3364–3373. doi:10.1111/j.1742-4658.2012.08608.x
30) Sparacino-Watkins, C., Stolz, J.F., Basu, P., 2013. Nitrate and periplasmic nitrate reductases. Chem. Soc. Rev. 43, 676. doi:10.1039/c3cs60249d
31) Spiro, S., Roberts, R.E., Guest, J.R., 2006. FNR-dependent repression of the ndh gene of *Escherichia coli* and metal ion requirement for FNR-regulated gene expression. Mol. Microbiol. 3, 601–608. doi:10.1111/j.1365-2958.1989.tb00207.x
32) Steuber, J., Krebs, W., Bott, M., Dimroth, P., 1999. A membrane-bound NAD(P)+-reducing hydrogenase provides reduced pyridine nucleotides during citrate fermentation by *Klebsiella pneumoniae*. J. Bacteriol. 181, 241–245.
33) Strohdeicher, M., Neuß, B., Bringer-Meyer, S., Sahm, H., 1990. Electron transport chain of *Zymomonas mobilis*. Arch. Microbiol. 154, 536–543. doi:10.1007/BF00248833
34) Wolfram Research, Inc., 2012. Mathematica. Wolfram Research, Inc.
35) Zhou, X., Shah, D.H., Konkel, M.E., Call, D.R., 2008. Type III secretion system 1 genes in *Vibrio parahaemolyticus* are positively regulated by ExsA and negatively regulated by ExsD. Mol. Microbiol. 69, 747–764. doi:10.1111/j.1365-2958.2008.06326.x

Figure Captions

Fig. 1. A) Cyclic voltammogram (1 mV/s) of neutral red (200 μM dissolved in 50 mM phosphate buffer, pH 6.0. Two reduction peaks were observed; the first at −560 $mV_{Ag/AgCl}$, the second at −910 $mV_{Ag/AgCl}$. Chronoamperometric polarization at −650$mV_{Ag/AgCl}$ and −950$mV_{Ag/AgCl}$ (corresponding to the orange #1 and teal #2 vertical lines in A) yielded two distinctly colored solutions with UV-visible spectra as shown in B).

Fig. 2. Lactate fermentation profiles for electrosynthesis (red) and control fermentation (black) for wild type *E. coli* K-12 (n = 4, reprinted with permission from Harrington et al., 2015), strain JW5536 (Δ*arcB*) (n=2) and strain JW5536 (pMMB207::*arcB*) (n=2). Electrosynthesis with wild type resulted in 5.52 mM higher production of lactate after 15.5 hours batch fermentation vs. control (P = 0.003). In the *arcB* knockout strain, there was no significant difference in lactate concentration between electrosynthesis and control at 15.5 hours (P = 0.6137). The growth of the *arcB* complement strain was extremely sensitive to IPTG concentration and the unusually early induction time, and restoration of wild-type fermentation profiles was unsuccessful. However, there was a 1.05 mM higher concentration of lactate (P = 0.05) for electrosynthesis vs. control in the complement strain at 15.5 hours.

Fig. 3. A) Current delivered to fermentation media containing 20 mM fumarate after inoculation into pre-reduced media with different strains of *E. coli* K-12 during electrosynthesis. B) Current delivered to media during batch electrosynthesis of wild type *E. coli* K-12 in the presence of pre-reduced neutral red and 20 mM of different anaerobic terminal electron acceptors.

Fig. 4. Proposed mechanism of neutral red-mediated electrosynthesis. Step 1: NRH^+ is reduced. Step 2: NRH_2 diffuses into the inner membrane. Step 3: NRH_2 is oxidized to NR (leuco-neutral red), with transfer of two electrons and two protons in the reduction of menaquinone (MK) to menaquinol (MKH_2). Step 4: NR diffuses out of the membrane to an ionic environment, where it picks up a proton (NRH^+). Step 5: Menaquinol diffuses in the membrane to the active site of a terminal reductase, where it may be oxidized with concomitant reduction of a terminal electron acceptor (OX: NO_3^-, NO_2^-,fumarate, DMSO, etc.) to its reduced product (RED: NO_2^-, NH_4, succinate, DMS, etc.). Step 6: Menaquinol reduces the arcB sensor kinase, initiating the cascade that results in phosphorylated arcA, which acts as a transcriptional regulator for multiple genes.

Tables and Figures

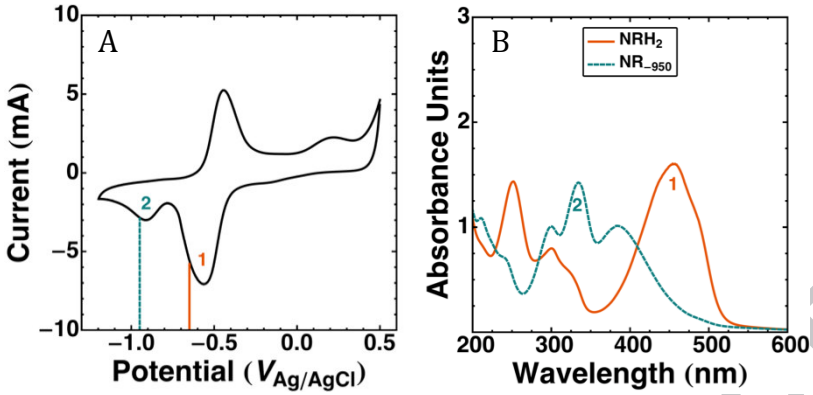

Fig. 1. A) Cyclic voltammogram (1 mV/s) of neutral red (200 µM dissolved in 50 mM phosphate buffer, pH 6.0. Two reduction peaks were observed; the first at −560 $mV_{Ag/AgCl}$, the second at −910 $mV_{Ag/AgCl}$. Chronoamperometric polarization at −650$mV_{Ag/AgCl}$ and −950$mV_{Ag/AgCl}$ (corresponding to the orange #1 and teal #2 vertical lines in A) yielded two distinctly colored solutions with UV-visible spectra as shown in B).

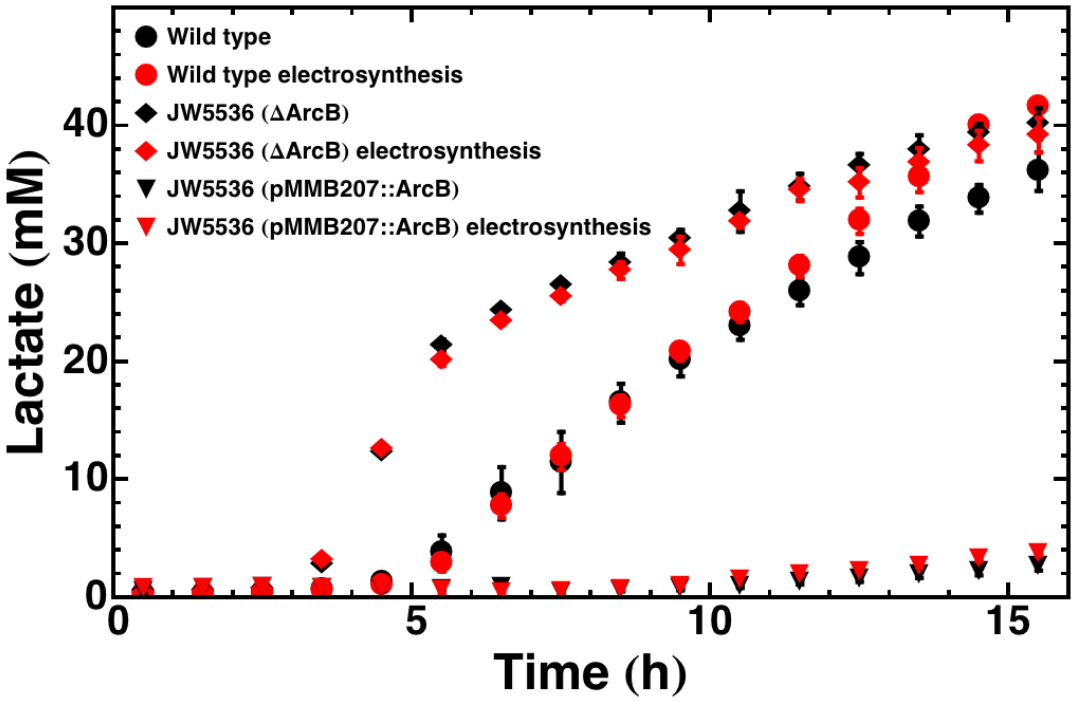

Fig. 2. Lactate fermentation profiles for electrosynthesis (red) and control fermentation (black) for wild type *E. coli* K-12 (n = 4, reprinted with permission from Harrington et al., 2015), strain JW5536 (Δ*arcB*) (n=2) and strain JW5536 (pMMB207::*arcB*) (n=2). Electrosynthesis with wild type resulted in 5.52 mM higher production of lactate after 15.5 hours batch fermentation vs. control (P = 0.003). In the *arcB* knockout strain, there was no significant difference in lactate concentration between electrosynthesis and control at 15.5 hours (P = 0.6137). The growth of the *arcB* complement strain was extremely sensitive to IPTG concentration and the unusually early induction time, and restoration of wild-type fermentation profiles was unsuccessful. However, there was a 1.05 mM higher concentration of lactate (P = 0.05) for electrosynthesis vs. control in the complement strain at 15.5 hours.

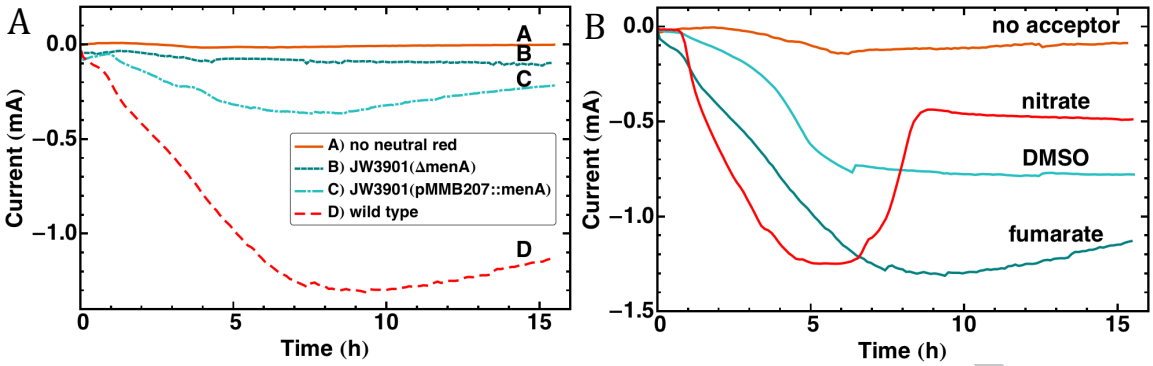

Fig. 3. A) Current delivered to fermentation media containing 20 mM fumarate after inoculation into pre-reduced media with different strains of *E. coli* K-12 during electrosynthesis. B) Current delivered to media during batch electrosynthesis of wild type *E. coli* K-12 in the presence of pre-reduced neutral red and 20 mM of different anaerobic terminal electron acceptors.

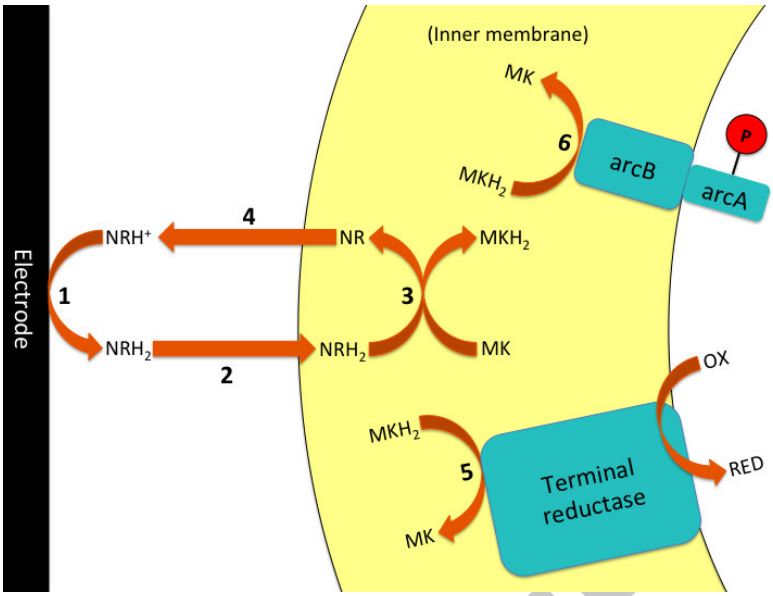

Fig. 4. Proposed mechanism of neutral red-mediated electrosynthesis. Step 1: NRH^+ is reduced. Step 2: NRH_2 diffuses into the inner membrane. Step 3: NRH_2 is oxidized to NR (leuco-neutral red), with transfer of two electrons and two protons in the reduction of menaquinone (MK) to menaquinol (MKH_2). Step 4: NR diffuses out of the membrane to an ionic environment, where it picks up a proton (NRH^+). Step 5: Menaquinol diffuses in the membrane to the active site of a terminal reductase, where it may be oxidized with concomitant reduction of a terminal electron acceptor (OX: NO_3^-, NO_2^-,fumarate, DMSO, etc.) to its reduced product (RED: NO_2^-, NH_4, succinate, DMS, etc.). Step 6: Menaquinol reduces the arcB sensor kinase, initiating the cascade that results in phosphorylated arcA, which acts as a transcriptional regulator for multiple genes.